Compressed CO_2 in AOT Reverse Micellar Solution: Effect on Stability, Percolation, and Size

Dong Shen, Buxing Han,* Yu Dong, Jiawei Chen, Tiancheng Mu, Weize Wu, and Jianling Zhang

The Center for Molecular Sciences, Institute of Chemistry, Chinese Academy of Sciences, Beijing 100080, China

Zhonghua Wu and Baozhong Dong

Institute of High Energy Physics, Chinese Academy of Sciences, Beijing 100039, China

Received: November 8, 2004; In Final Form: January 19, 2005

The effects of compressed CO_2 in sodium bis-2-ethylhexylsulfosuccinate (AOT)/decane reversed micellar solution on the stability of the micelles, interface, and micelle/micelle interactions were studied. It was demonstrated that the compressed gas could increase the solubilization of water in this system. The formation of the stabilized one-phase microemulsion was confirmed by conductivity measurements. A shift in percolation threshold to higher temperature was observed after compressed gas was added. The gyration radius (R_g) of the reverse micelles was determined using SAXS. R_g increases with the addition of water, while it decreases appreciably with increasing pressure of compressed gas at fixed W_0. These results were interpreted in terms of an increase of the rigidity of the interface layer and a decrease of the interdroplet attraction. The results of this work provide useful information to get insight into the mechanism of cosurfactants to stabilize reverse micelles.

Introduction

Reverse micelles or water-in-oil microemulsions are generally described as nanometer-sized water droplets dispersed in an apolar solvent with the aid of a surfactant monolayer, forming a thermodynamically stable and optically transparent solution.[1] It is well-established that phase separation of reverse micelles can arise from either interdroplet interactions or greater curvatures than the natural curvature of the interface for water-in-oil micelles.[2−4] In the micelle−micelle interactions mechanism, attractive forces due to overlap between the tails of neighboring reverse micelles cause surfactant and water to precipitate into a new surfactant-rich phase.[5,6] In the natural curvature mechanism, relatively pure excess water precipitates when the micelle radius becomes equal to the natural curvature.[4] The one-phase region in a temperature versus W_0 ($W_0 = [H_2O]/[\text{surfactant}]$) diagram of a nonionic surfactant in oil system extends to large W_0 values over a narrow temperature interval.[7−9] It is known that the lower boundary of the one-phase region results from the micelle−micelle interactions. It is usually called the haze point boundary or solubility curve. Phase separation at the upper boundary is caused by natural curvature mechanism. It is called the solubilizaton curve, in reference to the solubilization of water. It should be noted that the position of the solubilization curve and solubility curve for anionic surfactant was opposite to that for nonionic surfactants.[10]

It is well-known that some compressed gases, such as CO_2 and ethylene, are quite soluble in a number of organic solvents and that they can reduce the solvent strength of the solvents to such a degree that the solutes can be precipitated. This process is usually referred to as gas antisolvent process (GAS).[11,12] Surprisingly, in the previous reports, we found that, at suitable pressure, compressed CO_2 could increase the solubilization capacity of water in AOT (sodium bis-2-ethylhexyl sulfosuccinate) and Triton X-100 reverse micellar systems as the systems are dominated by micelle−micelle interactions mechanism.[13,14] We deduced that the compressed gas could stabilize the reverse micelles by decreasing the attractive interdroplet interaction of micelles. However, further detailed studies are required.

The electrical conductivity measurements constitute a very useful technique for obtaining information about micellar interactions.[15−22] A microemulsion has a very low conductivity, 10^{-9} to 10^{-7} Ω^{-1} cm^{-1}. However, this is much larger than the conductivity of alkanes (ca. 10^{-14} Ω^{-1}) and is due to the fact that micelles carry charges. A well-known phenomenon occurs when water is added to the system: at a certain volume fraction, the conductivity rises sharply over a narrow range and then remains practically unchanged at a considerably higher value than before the transition. A similar behavior is observed if the temperature is increased keeping the composition constant. This phenomenon is called percolation. It is usually considered that during percolation the droplets come in contact and ions are transferred by some kind of hopping mechanism and/or channels are formed through which micellar content can be exchanged; the conductance is, thus, greatly enhanced after a threshold level.[21]

From the theoretical point of view, two different approaches have been proposed for the mechanism leading to percolation.[18] The first model, static percolation, attributes the observed phenomena to the transformation into a bicontinuous structure, whereas the dynamic percolation model postulates the attractive interaction between droplets leading to cluster formation and

* Corresponding author. Phone: 86-10-62562821. Fax: 86-10-62562821. E-mail: hanbx@iccas.ac.cn.

10.1021/jp044874+ CCC: $30.25
Published on Web 03/03/2005

thus causes an increase in the microemulsion conductivity. W/O microemulsions formed with AOT have been shown to exist as discrete water droplets in oil. The cluster model was therefore widely used for such systems in recent years.[23,24]

For percolation to occur in the AOT/decane system, micelles must cluster, and any alteration in this process caused by addition of additives or cosurfactants will be reflected in the percolating temperature. To further demonstrate the effect of addition of CO_2 on the attractive interdroplet interaction, in the present paper, the effect of compressed CO_2 on temperature-induced percolation of AOT reverse micelles was studied. In addition, the gyration radii R_g of the AOT reverse micelles in the presence of compressed CO_2 were determined using small-angle X-ray scattering.

Experimental Procedures

Materials. AOT of 99% purity was purchased from Sigma; decane (99%) was provided by Acros. CO_2 (99.995% purity) was supplied by Beijing Analytical Instrument Factory. All the reagents were used without further purification. Double distilled water was used.

Conductivity Measurements. The conductivity of the reverse micelles in the presence of compressed CO_2 was measured as a function of temperature and W_0 (water-to-AOT molar ratio). The apparatus was similar to those reported previously.[25] It consisted mainly of a high-pressure stainless steel vessel, a conductivity cell, a constant temperature water bath, a high-pressure syringe pump, a pressure gauge, a magnetic stirrer, and a gas cylinder. The temperature of the water bath was controlled using a Haake-D8 controller. The pressure gauge was composed of a pressure transducer (FOXBORO/ICT, Model 93) and an indicator, which was accurate to 0.025 MPa in the pressure range of 0−20 MPa. Both working electrode and counter electrode of the conductivity cell were made of 0.3 mm thick Pt foil. The conductivity was determined by a conductivity meter with a precision of 1%, which was produced by Shanghai Precision Scientific Instrument Co., LTD (DDS-307). The cell constant was calibrated with KCl aqueous solutions at various temperatures. In a typical experiment, the stainless steel vessel was flushed with CO_2 to remove the air. A suitable amount of double distilled water and the AOT/decane solution was charged into the stainless steel vessel. The sealed stainless steel vessel was placed into the constant temperature water bath of desired temperature. After thermal equilibrium had been reached, CO_2 was charged into the system until the desired pressure was reached, and the magnetic stirrer started to facilitate the dissolution of CO_2 in the solution. The conductivity of the solution at equilibrium was determined, and equilibrium was confirmed by the facts that both the pressure and the conductivity were independent of equilibration time. The temperature was raised, and the conductivity was determined. All the experiments were conducted in the single-phase region of the mixture.

SAXS Experiments. SAXS experiments were carried out at Beamline 4B9A at the Beijing Synchrotron Radiation Facility (BSRF). The small-angle X-ray scattering station was located 31 m from the source. The station was equipped with a SAXS camera, a detector, an on-line data-acquisition, a controlling system, and an alignment carriage. The data accumulation time was 3 min. The wavelength used was 1.54 Å, and the sample-to-detector distance was 1.510 m. The detailed description of the spectrometer was given elsewhere.[26] The high-pressure SAXS cell was the same as that used previously.[27] It was composed mainly of a stainless steel body and two diamond windows of 8 mm in diameter and 0.4 mm in thickness. The cell body was coiled with an electric heater and heat-insulation ribbon outside, which was electrically heated to 0.1 K of the desired temperature by using a temperature controller with a platinum resistance temperature probe (Model XMT, produced by Beijing Chaoyang Automatic Instrument Factory). The X-ray path length of the cell was 1.5 mm, and the internal volume of the cell was 2.7 cm^3. The high-pressure pump was model DB-80, which was used for charging CO_2 into the system. The accuracy of the pressure gauge was the same as described previously.

In a typical experiment, the air in the sample cell was replaced by CO_2. The desired amount of AOT/decane solution and double distilled water was added into the sample cell. After the system had reached thermal equilibrium, CO_2 was pumped into the cell until the desired pressure was reached. The cell was connected to the apparatus after enough equilibration time, and the X-ray scattering was recorded.

SAXS Data Analysis. The Guinier approximation was often used to obtain the size of the reverse micelles.[28,29] This approximation is based on the fact that the scattering curve shows Gaussian shape at small angles, of which the slope depends on the radius of gyration. After correction of the scattering data by subtraction of the background noise, the following analyses were done. In the lower q region, contributions to the total excess X-ray scattering, $I(q)$, due to microemulsions can rise from two sources: the droplet contribution, which depends solely upon the radius of the droplet, and an appropriate structure factor, which accounts for attractive or repulsive interactions between the droplets. When the system is sufficiently dilute, interdroplet interactions are negligible. The magnitude of the scattering vector q is given in terms of the scattering angle θ by $q = 4\pi \sin\theta/\lambda$, where λ is the incident X-ray wavelength of 1.54 Å. For dilute solutions, the gyration radius R_g of the micellar core can be obtained by using the Guinier approximation law, which is valid at a low q region and can be expressed by eq 1.[28, 29]

$$\ln[I(q)] = \ln[I(0)] - \frac{(qR_g)^2}{3} \tag{1}$$

where $I(0)$ denotes the scattering intensity extrapolated to zero angle. The Guinier plots give a precise value of the gyration radius only if the representation is linear at small values of q. In this work, by using Guinier plot ($\ln I(q)$ vs q^2) on the data sets in a defined small q range (0.022 to ~0.031 $Å^{-1}$), linear regression analysis of the intensity curves were used to obtain R_g values. The true radius of spherical micelles (R_c) is obtained by eq 2.

$$R_c = \sqrt{\frac{5}{3}} R_g \approx 1.29\, R_g \tag{2}$$

Results and Discussion

Electrical Conductivity in the Presence of Compressed CO_2. In the previous studies, we found that compressed CO_2 could enhance the stability of AOT/larger alkanes microemulsions and then increase the solubilization of water when the temperature was at or above room temperature.[14] In this paper, we further determined the value of W_0 as a function of pressure of compressed CO_2 in decane/AOT reverse micelles system at 30 °C, and the results are shown in Figure 1. In the absence of compressed CO_2, phase separation occurs when the value of W_0 is above 40. However, the maximum value of W_0 (W_0^{max}) can reach about 72 at appropriate CO_2 pressure. The microemulsion can be separated into two phases simply by decreasing

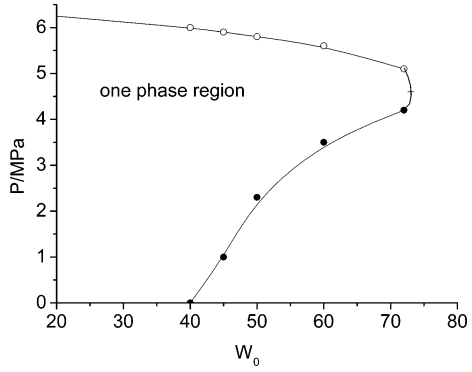

Figure 1. W_0 as a function of CO_2 pressure in AOT/decane system at 30.0 °C (C_{AOT} = 0.1 mol/L).

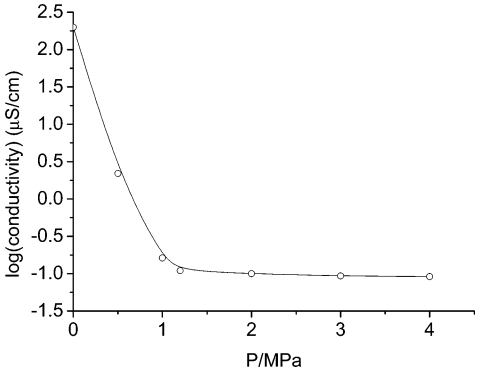

Figure 2. Conductivity as a function of CO_2 pressure in AOT/decane system at 30.0 °C (C_{AOT} = 0.2 mol/L and W_0 = 35).

or increasing the pressure of CO_2, and a homogeneous one-phase microemulsion forms again when the CO_2 pressure is adjusted.

The conductivity as a function of added water was also determined in the presence of compressed CO_2 within the one-phase region. It was found that, at suitable pressure (P = 4.5 MPa), the conductivity values remained below 0.3 μS/cm until the system separated into two phases. This suggests that stabilized one-phase microemulsion can be formed with the assistance of compressed CO_2.

As the volume fraction of water droplets increases, attractive interdroplet interactions increase, leading to droplet clustering and thus resulting in a sharp increase of electric conductivity in reverse micelles system.[30] In our experiments, the electric conductivity increased abruptly when W_0 is above 32 in the absence of the compressed gas. This indicates the formation of the droplet cluster at this condition. However, an obvious decrease in conductivity was found when compressed CO_2 was added to this system (Figure 2). The conductivity remains unchanged as the pressure is higher than about 1 MPa, and the conductivity is equal to that for the microemulsions before the percolation occurs. This phenomenon indicates that the addition of compressed CO_2 can decrease the attractive interdroplet interaction between adjacent micelles effectively.

Temperature-Induced Percolation in AOT/Decane Reverse Micelle System. Percolation is a known phenomenon in which, at a certain volume fraction of the dispersed phase (at constant temperature) or a certain temperature (at constant composition), there is a sharp increase in the usually low conductivity of the reverse micelle, which can span 3 or 4 orders of magnitude. This phenomenon is usually envisaged as micelles clustering and aggregating so that charged material can be exchanged between them. The percolation temperature is defined here as the point at which a dramatic change in slope in the

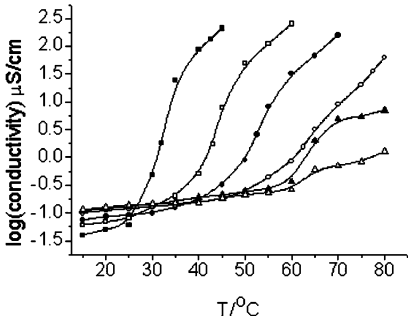

Figure 3. Conductivity as a function of temperature for water-in-decane reverse micelle at various CO_2 pressures (■ P = 0, □ P = 1.0, ● P = 2.0, ○ P = 3.0, ▲ P = 4.0, △ P = 4.6, and T = 15 °C) at W_0 = 20 and C_{AOT} = 0.2 mol/L.

conductivity versus temperature curve occurs. As the temperature is increased, there is an increase in the interfacial flexibility, resulting in shape fluctuations and then clustering and percolation.[1]

Most of the literature involving percolation is related to percolation induced by the addition of water[31−35] or by the addition of nonaqueous solvents (i.e., volume fraction-induced percolation).[36] Alexandridis et al.[21] did a comprehensive study of temperature-induced percolation in AOT water-in-oil microemulsions, studying the effect of solvent, W_0, and micelle concentration. The authors concluded that the percolating temperature decreased with the increase in water content, micelle concentration, and molecular weight of the solvent and also concluded that the percolating process is enthalpically disfavored.

Over the past decade, a number of studies has been carried out to analyze the effect of additives on the mechanism of dynamic percolation.[37−45] Hurugen et al.[46] studied the effect of cytochrome *c* on the percolating process and concluded that percolation occurs at room temperature in the presence of their solubilizate. Moulik et al.[20] used temperature-induced percolation to study the effect of alcohols, cholesterol, and crown ether on the percolating temperature. The results demonstrate that alcohols and cholesterol increase the percolating temperature and that crown ethers decrease it. Nazario et al.[1] studied the effect of nonionic cosurfactants on temperature-induced percolation for several quaternary systems. It was found that poly(oxyethylene) alkyl ethers (C_iE_j) shift the percolation to lower temperature. In addition, the phase behavior and electrical conductivity of water-in-carbon dioxide (W/C) microemulsions are reported over a range of temperatures, pressures, and droplet volume fractions. The scaling analysis of the conductivity data supports a dynamic percolation model, whereby the attractive interdroplet interactions form clusters of discrete droplets with rapid charge transport.[30,47]

As percolation is dependent on the clustering of reverse micelles, anything that might promote or reduce clustering will obviously have an implication on the percolation process. We further investigated the effect of compressed CO_2 on the percolating temperature in the AOT/decane system (Figure 3). As W_0 is less than 10, the logarithm of the reverse micelles conductivity increases linearly with temperature for all droplets concentrations studied, which does not suggest a percolation process.[21] Moreover, it is difficult to determine a percolating temperature because the stability boundary of the single phase is reached as the concentration of AOT is too dilute. Therefore, C_{AOT} = 0.2 mol/L and W_0 = 20 was selected in our experiments.

It can be seen from Figure 3 that the system has a higher percolating temperature when compressed CO_2 is added, and

TABLE 1: Values of the Scaling Exponents μ and s Obtained at Different CO_2 Pressures

P (Mpa)	0	1.0	2.0	3.0
s	1.17 ± 0.11	1.04 ± 0.07	1.07 ± 0.08	0.99 ± 0.09
μ	1.75 ± 0.12	1.80 ± 0.13	1.81 ± 0.11	1.83 ± 0.14

the higher pressure of the gas results in the higher percolating temperature. For the AOT reverse micellar system, the scaling laws of the percolation theory have been applied.[30,48,49]

$$\sigma = C_1\sigma_1(\phi - \phi_p)^{\mu} \quad (3)$$

$$\sigma = C_2\sigma_2(\phi_p - \phi)^{-s} \quad (4)$$

In eqs 3 and 4, C_1 and C_2 are prefactor terms, whereas σ_1 and σ_2 correspond to the conductivity of the droplets and the continuous phase, respectively. ϕ and ϕ_p stand for the volume fraction of droplets and volume fraction of droplets at the percolation threshold, respectively. Percolation with temperature can be understood in terms of the dynamic percolation model by considering the fact that ϕ_p is a function of T and W_0. The percolation threshold temperature T_p is defined as the temperature at which $\phi = \phi_p$ and is determined in a similar manner as ϕ_p (i.e., the point of inflection on a log of conductivity vs temperature plot). Thus, the effect of changing the temperature on microemulsion conductivity, to a first-order approximation, is given by

$$\sigma = C_1\sigma_1[-K(T - T_p)]^{\mu} \quad (T > T_p) \quad (5)$$

$$\sigma = C_2\sigma_2[-K(T_p - T)]^{-s} \quad (T < T_p) \quad (6)$$

In AOT microemulsion systems, K is independent of temperature, and the scaling exponents μ and s can be determined from the plots of the log of conductivity versus the log of $(T - T_p)$ and $(T_p - T)$, respectively. In the presence of compressed CO_2, the results for the scaling exponent were listed in Table 1.

The results are consistent with the values expected from the dynamic percolation model and those obtained for the water/AOT/liquid alkane systems ($\mu \approx 1.7$ and $s \approx 1.2$) in the absence of compressed CO_2.[50,51] Thus, the increase in electrical conductivity in the CO_2 assisted reverse micellar system is likely due to the clustering of discrete droplets from attractive interdroplet interactions.

For AOT/oil systems with larger alkane solvents, it is well-known that the decrease of the solubilization capacity of water is due to an increase in the attractive interactions between droplets. Hou et al.[2] reported that the interdroplet attractive interaction in AOT water-in-oil microemulsons increased significantly with increasing W_0 and chain length of the alkane solvents. Small-angle neutron scattering experiments in quaternary microemulsion systems also showed that the magnitude of the attractive interaction between the microemulsion droplets increased as the alkane solvent chain length increased.[19] An increase in the droplet radius would increase the overlap volume between two droplets, and consequently, the interaction potential. Percolation can thus be facilitated.[52] While droplet attractions play an important role in percolation, the nature of the interface of the individual droplets also affects percolation. Droplets must exchange contents and so the droplet interface must rupture. Jada[17,35] and Alexandridis[21] found that the percolation threshold decreased as the apolar solvent chain length increased in AOT microemulsion systems. This was attributed to a reduction in solvent penetration into the interface of the droplet with increasing solvent molecular weight, resulting in greater interdroplet attraction and lower percolating temperature.

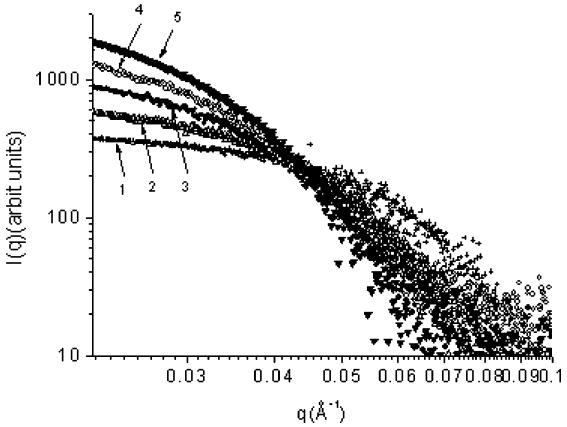

Figure 4. SAXS curves of AOT/decane reverse micelle solutions with various W_0 in the presence of compressed CO_2 ($P = 4.5$ MPa, $C_{AOT} = 0.1$ mol/L, and $T = 30$ °C). (1) $W_0 = 20$, (2) $W_0 = 35$, (3) $W_0 = 50$, (4) $W_0 = 60$, and (5) $W_0 = 70$.

As percolation is directly related to micelle clustering and the attractive interactions, one can conclude that compressed CO_2 makes clustering more difficult and decreases the attractive interactions between droplets. McFann et al. studied the phase behavior of AOT−alkane−brine systems at different conditions for alkanes from ethane to dodecane.[53] They concluded that a small solvent like propane penetrates the surfactant tails very well, although its attractive interactions with the tails are too weak to prevent tail−tail interaction. Since CO_2 is quite soluble in decane, we can expect that they can penetrate into the micellar interface; their effect on clustering is mainly due to the changes of the properties of the interface. It is most likely that CO_2 solubilizes in the surfactant tail region and so pushes the surfactant headgroups together and then increases the rigidity of the interface. In view of the percolation temperature, the resulting conclusion is that compressed CO_2 makes the interface more rigid and hence makes clustering and percolation more difficult. It was well-established that the solubilization capacity of AOT reverse micelles is limited by a smaller critical droplet radius (R^c) as the phase separation is governed by the micelle−micelle attractive interaction mechanism.[4] A more rigid interface will decrease the attractive interaction between droplets and then increase the solubilization of water in the AOT/decane system by increasing the critical droplet radius (R^c).

In comparison with the works of other authors,[1,20] we can find that the small nonpolar gaseous molecules and alcohols have the similar effect on the percolating temperature. This may imply that compressed CO_2 has the same function as alcohol cosurfactants in respect to enhancement the stability of reverse micelles when the reverse micelles formed fall in the range where attractive interaction is important.

SAXS Study. It is well-known that SAXS is a useful technique to provide the information about the microstructure of reverse micelles. To investigate the size of the micelle formed in the presence of compressed CO_2, SAXS experiments were carried out in this work. The effect of the experimental conditions on the scattering intensity and the gyration radii (R_g) was studied at different W_0 values. The SAXS curves of reverse micelle solutions with various W_0 values in the presence of compressed CO_2 are shown in Figures 4 and 5.

Figure 4 shows that in the small angle region the scattering intensity gradually increases with the increase of W_0. This

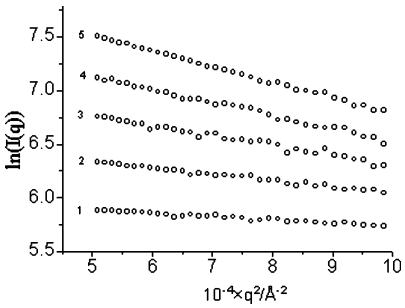

Figure 5. Guinier plots of AOT/decane reverse micelle solutions with various W_0 in the presence of compressed CO_2 ($P = 4.5$ MPa, $C_{AOT} = 0.1$ mol/L, and $T = 30$ °C). (1) $W_0 = 20$, (2) $W_0 = 35$, (3) $W_0 = 50$, (4) $W_0 = 60$, and (5) $W_0 = 70$.

TABLE 2: Gyration Radius *R*g of AOT/Decane Reverse Micelle at Various W_0 in the Presence of Compressed CO_2[a]

W_0	20	35	50	60	70
R_g (Å)	29.7	42.8	53.7	61.3	65.7

[a] $P = 4.5$ MPa, $C_{AOT} = 0.1$ mol/L, and $T = 30$ °C.

variation likely results from the enlargement of the micellar dimension induced by the increasing solubilization of water. The Guinier plots of $q^2 \sim \ln I(q)$ in the presence of CO_2 show linearity in the q^2 range of 0.0005−0.0010 (Figure 5). The gyration radii (R_g) of the reverse micelles at different conditions are estimated using eq 1, and the corresponding R_g of the reverse micelles at different W_0 values is shown in Table 2. It can be known from Table 2 that R_g increases continuously with the increase of the W_0 value. It is easy to understand that the size of the micellar core increases with increasing W_0 at constant concentration of AOT. These results confirm the conductivity results in Figure 2 (i.e., AOT/decane solution saturated with CO_2 form aggregates similar to those in the absence of CO_2).

Moreover, a linear true radius of spherical micelles (R_c) (obtained by eq 2) versus W_0 relationship is obtained at $20 \leq W_0 \leq 60$. This linear behavior can be used to estimate the headgroup area per surfactant molecular at the water−oil interface (a_h) using the following equation[54,55]

$$\alpha(p)R_c = \frac{3\nu_W}{\alpha_h}w_0 + \frac{3\nu_h}{\alpha_h} \qquad (7)$$

where υ_w is the volume of a water molecule, υ_h is the volume of the water-penetrated portion of a single AOT headgroup, p is the polydispersity index (σ/R_c), and $\alpha(p)$ depends on the particular functional form of this distribution. In this work, a_h was estimated and to be 88 ± 2 Å^2 at higher CO_2 pressure (4.5 Mpa). The current result is slightly higher than that of AOT at the water−alkane interfaces (about 65 ± 5 Å^2) in the absence of CO_2.[29,54] As pointed out by Kotlarchyk,[55] a_h in the AOT/decane microemlusion increases as the temperature decreases. The decrease of temperature will lead to a decrease in the interfacial flexibility and thus makes clustering more difficult. Therefore, the slight increase of a_h in the presence of CO_2 further confirms the conductivity results discussed in the previous section (i.e., the addition of CO_2 has a similar effect as decreasing temperature). It can decrease the attractive interactions between droplets, make clustering more difficult, and consequently, the percolating temperature is moved toward higher temperatures.

As discussed previously, the effects of compressed CO_2 on micelle−micelle interactions and on the micellar interface have been related to an increase of the interfacial rigidity. A change

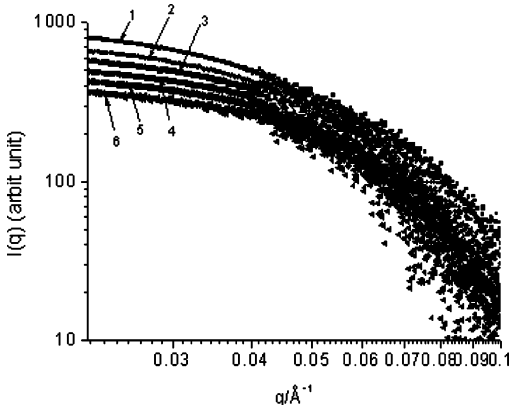

Figure 6. SAXS curves of AOT/decane reverse micelle solutions at various CO_2 pressures at $W_0 = 20$. $C_{AOT} = 0.1$ mol/L and $T = 30$ °C. (1) $P = 0$ MPa, (2) $P = 1.0$ MPa, (3) $P = 2.0$ MPa, (4) $P = 3.0$ MPa, (5) $P = 4.0$ MPa, and (6) $P = 4.5$ MPa.

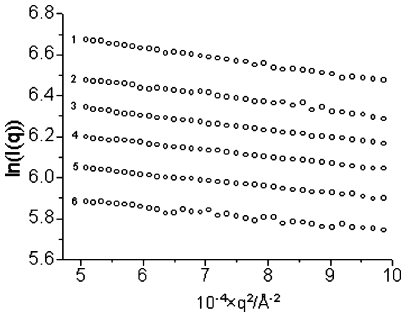

Figure 7. Guinier plots of of AOT/decane reverse micelle solutions at various CO_2 pressures at $W_0 = 20$. $C_{AOT} = 0.1$ mol/L and $T = 30$ °C. (1) $P = 0$ MPa, (2) $P = 1.0$ MPa, (3) $P = 2.0$ MPa, (4) $P = 3.0$ MPa, (5) $P = 4.0$ MPa, and (6) $P = 4.5$ MPa.

TABLE 3: Effect of Compressed CO_2 Pressure on the Gyration Radius R_g of AOT/Decane Reverse Micelle

P (Mpa)	0	1.0	2.0	3.0	4.0	4.5
*R*g (Å)	35.7	34.2	32.8	31.5	30.3	29.7

[a] $C_{AOT} = 0.1$ mol/L, $T = 30$ °C, and $W_0 = 20$.

in the fluidity of the interface should have an effect on the size of the individual micelles, and an increase in rigidity should make shape fluctuations less favorable. Therefore, we further investigated the effect of CO_2 pressure on the R_g of the reverse micelles at constant W_0 (Figures 6and 7and Table 3). With the increase of CO_2 pressure, in the small angle region, the scattering intensity decreases appreciably (Figure 6), and the obtained R_g values of the reverse micelles also gradually decrease (Table 3). These results are consistent with that obtained from the CO_2-dissolved AOT/water/isooctane reverse micelles (i.e., the micellar core decreases with increasing CO_2 pressure).[56] Other authors[1] found that the presence of alcohol has a major effect on the apparent hydrodynamic radius (r_h^a) of the AOT reverse micelles and that the r_h^a decreases as the concentration of the alcohol in the system is increased. Our results further indicate that compressed CO_2 can make the micellar interface more rigid, reduce the shape fluctuations, and then decrease the dimension of micelles. The possible reason is that compressed CO_2 solubilizes in the surfactant tail region and so pushes the surfactant headgroups together and then increases the micellar curvature.

A conventional cosurfactant (usually an alcohol) contains both a polar group and a hydrocarbon chain, and it is very difficult to clarify the functions of its polar group and the hydrocarbon chain. The results of this work suggest that compressed CO_2

has the function of cosurfactant, while the gas is a small nonpolar molecule, which solely has the function of the hydrocarbon chain in a cosurfactant. Therefore, the results of this work indicate that the chain of a cosurfactant can stabilize the reverse micelles. This is useful information to obtain insight into the mechanism of cosurfactants to stabilize reverse micelles.

Conclusion

The effect of compressed CO_2 on the stability of AOT reverse micelles in decane has been studied using electric conductivity measurement and small-angle X-ray scattering technique. It was found that the compressed gas could increase the solubilization of water considerably, and the stabilized one-phase microemulsion was formed. Conductivity percolation takes place when microemlusion droplets come close enough so that ions can hop from one to another and/or when droplets coalesce and exchange materials. An increase in temperature would result in an increase in the interfacial flexibility, which will favor interactions and shape fluctuations and facilitate clustering. Compressed CO_2 used in this study penetrates into the surfactant tail region, pushing the surfactant heads together and so increasing the curvature and rigidity and then increases the percolation temperature. As the phase separation is governed in by micelle−micelle attractive interaction mechanisms, a rigid interface results in a decrease in droplet interaction and, consequently, increases the stability of the micelles and the amount of the solubilized water.

Acknowledgment. The authors are grateful to the National Natural Science Foundation of China (20133030) and Ministry of Science and Technology for the financial support (G2000078103).

References and Notes

(1) Nazario, L. M. M.; Hatton, T. A.; Crespo, J. P. S. G. *Langmuir* **1996**, *12*, 6326.
(2) Hou, M. J.; Kim, M.; Shah. D. O. *J. Colloid Interface Sci.* **1988**, *123*, 398.
(3) Leung, R.; Shah, D. O. *J. Colloid Interface Sci.* **1987**, *120*, 330.
(4) Hou, M. J.; Shah, D. O. *Langmuir* **1987**, *3*, 1086.
(5) Roux, D.; Bellocq, A. M.; Bothorel, P. *Surfactant in Solution*, Vol. 3; Mittal, K. L., Lindman, B., Eds.; Plenum: New York, 1984.
(6) Peck, D. G.; Johnston, K. P. *J. Phys. Chem.* **1993**, *97*, 5661.
(7) Kon-no, K.; Kitahara, A. *J. Colloid Interface Sci.* **1970**, *34*, 221.
(8) Shinoda, K.; Ogawa, T. *J. Colloid Interface Sci.* **1967**, *24*, 56.
(9) Aveyard, R.; Binks, B. P.; Fletcher, P. D. I. *Langmuir* **1989**, *5*, 1209.
(10) Kon-no, K.; Kitahara, A. *J. Colloid Interface Sci.* **1971**, *37*, 469.
(11) McHugh, M. A.; Krukonis, V. J. *Supercritical Fluids Extraction: Principles and Practice*, 2nd ed.; Butterworth-Heinemann: Stoneham, MA, 1994.
(12) Eckert, C. A.; Barbara, L. K.; Debenedetti, P. G. *Nature* **1996**, *383*, 313.
(13) Shen, D.; Zhang, R.; Han, B. X.; Dong, Y.; Wu, W. Z.; Zhang, J. L.; Li, J. C.; Jiang, T.; Liu, Z. M. *Chem.−Eur. J.* **2004**, *10*, 5123.
(14) Shen, D.; Han, B. X.; Dong, Y.; Wu, W. Z.; Chen, J. W.; Zhang, J. L. *Chem.−Eur. J.* **2005**, *11*, 1228.
(15) Velázquez, M. M.; Valero, M.; Ortega, F. *J. Phys. Chem.* **2001**, *105*, 10163.
(16) Maitra, A.; Mathew, C.; Varshney, M. *J. Phys. Chem.* **1990**, *94*, 5290.
(17) Jada, A.; Lang, J.; Zana, R. *J. Phys. Chem.* **1989**, *93*, 10.
(18) Ponton, A.; Bose, T. K.; Delbos, G. *J. Chem. Phys.* **1991**, *94*, 6879.
(19) Hamilton, R. T.; Billman, J. F.; Kaler, E. W. *Langmuir* **1990**, *6*, 1696.
(20) Mukhopadhyay, L.; Bhattacharya, P. K.; Moulik, S. P. *Colloids Surf.* **1990**, *50*, 295.
(21) Alexandridis, P.; Holzwarth, J. F.; Hatton, T. A. *J. Phys. Chem.* **1995**, *99*, 8222.
(22) Dasilva-Carvalhal, J.; Garcia-Rio, L.; Gomez-Diaz, D.; Mejuto, J. C.; Rodriguez- Dafonte, P. *Langmuir* **2003**, *19*, 5975.
(23) Koper, G. J. M.; Sager, W. F. C.; Smeets, J.; Bedeaux, D. *J. Phys. Chem.* **1995**, *99*, 13291.
(24) Holger, M. *J. Phys. Chem.* **1997**, *101*, 10271.
(25) Zhang, J. M.; Yang, C. H.; Hou, Z. S.; Han, B. X. *New J. Chem.* **2003**, *27*, 333.
(26) Dong, B. Z.; Sheng, W. J.; Yang, H. L.; Zhang, Z. J. *J. Appl. Cryst.* **1997**, *30*, 877.
(27) Li, D.; Han, B. X.; Liu, Z. M.; Liu, J.; Zhang, X. G.; Wang, S. G.; Zhang, X. F. *Macromolecules* **2001**, *34*, 2195.
(28) Hirai, M.; Kawai-Hirai, R.; Yabuki, S.; Takizawa, T.; Hirai, T.; Kobayashi, K.; Amemiya, Y.; Oya, M. *J. Phys. Chem.* **1995**, *99*, 6652.
(29) Hirai, M.; Kawai-Hirai, R.; Sanada, M.; Iwase, H.; Mitsuya, S. *J. Phys. Chem. B* **1999**, *103*, 9658.
(30) Lee-Jr, C. T.; Bhargava, P.; Johnston, K. P. *J. Phys. Chem. B* **2000**, *104*, 4448.
(31) Lagues, M.; Ober, R.; Tauprin, C. *J. Phys. Lett.* **1978**, *39*, 487.
(32) Van-Dijk, M. A. *Phys. Rev. Lett.* **1985**, *55*, 1003.
(33) Lagues, M.; Sauteray, C. *J. Phys. Chem.* **1980**, *84*, 3503.
(34) Ninham, B. W.; Chen, S. J.; Fennell-Evans, D. *J. Phys. Chem.* **1984**, *88*, 5855.
(35) Jada, A.; Lang, J.; Zana, R. *J. Phys. Chem.* **1990**, *94*, 381.
(36) Ray, S.; Bisal, S. R.; Moulik, S. P. *J. Chem. Soc., Faraday Trans.* **1993**, *89*, 3277.
(37) Schubel, D.; Ilgenfritz, G. *Langmuir* **1997**, *13*, 4246.
(38) Kahlweit, M.; Strey, R.; Busse, G. *J. Phys. Chem.* **1990**, *94*, 3881.
(39) Amaral, C. L. C.; Brino, O.; Chaimovich, H.; Politi, M. J. *Langmuir* **1992**, *8*, 2417.
(40) Adachi, M.; Harada, M.; Shioi, A.; Sato, Y. *J. Phys. Chem.* **1991**, *95*, 7925.
(41) Garcia-Rio, L.; Herves, P.; Leis, J. R.; Mejuto, J. C. *Langmuir* **1997**, *13*, 6083.
(42) Schuebel, D. *Colloid Polym. Sci.* **1998**, *276*, 743.
(43) Moulik, S. P.; De, G. C.; Bhowmik, B. B.; Panda, A. K. *J. Phys. Chem. B* **1999**, *103*, 7122.
(44) Hait, S. K.; Moulik, S. P.; Rodgers, M. P.; Burke, S. E.; Palepu, R. *J. Phys. Chem. B* **2001**, *105*, 7145.
(45) Hait, S. K.; Moulik, S. P. *J. Phys. Chem. B* **2002**, *106*, 12642.
(46) Hurugen, J. P.; Authier, M.; Greffe, J. L.; Pileni, M. P. *Langmuir* **1991**, *7*, 243.
(47) Nagashima, K.; Lee-Jr, C. T.; Xu, B.; Johnston, K. P.; DeSimone, J. M.; Johnson, C. S., Jr. *J. Phys. Chem. B* **2003,** *107*, 1962.
(48) Grest, G. S.; Webman, I.; Safran, S. A.; Bug, A. L. R. *Phys. Rev. A* **1986**, *33*, 2842.
(49) Peyrelasse, J.; Boned, C. *Phys. Rev. A* **1990**, *41*, 938.
(50) Bhattacharya, S.; Stokes, J. P.; Kim, M. W.; Huang, J. S. *Phys. Rev. Lett.* **1985**, *55*, 1884.
(51) Kim, M. W.; Huang, J. S. *Phys. Rev. A* **1986**, *34*, 719.
(52) Lemaire, B.; Bothorel, P.; Roux, D. *J. Phys. Chem.* **1983**, *87*, 1023.
(53) McFann, G. J.; Johnston, K. P. *J. Phys. Chem.* **1991**, *95*, 4889.
(54) Nave, S.; Eastoe, J.; Heenan, R. K.; Steytler, D. C.; Grillo, I. *Langmuir* **2000**, *16*, 8741.
(55) Kotlarchyk, M.; Chen, S.-H.; Huang, J. S. *J. Phys. Chem.* **1982**, *86*, 3273.
(56) Zhang, J. L.; Han, B. X.; Liu, J. C.; Zhang, X. G.; Yang, G. Y.; He, J.; Liu, Z. M.; Jiang, T. *J. Chem. Phys.* **2003**, *118*, 3329.